



Review

An Effective Utilization of Solar Energy: Enhanced Photodegradation Efficiency of TiO₂/Graphene-Based Composite

Peipei Huo ¹ , Peng Zhao ², Yin Wang ³, Bo Liu ^{1,*} and Mingdong Dong ^{3,*} 

¹ Laboratory of Functional Molecules and Materials, School of Physics and Optoelectronic Engineering, Shandong University of Technology, Xincun West Road 266, Zibo 255000, China; peipeihuo@sdut.edu.cn

² School of Materials Science and Engineering, Shandong University of Technology, Xincun West Road 266, Zibo 255000, China; 16509140463@stumail.sdut.edu.cn

³ Interdisciplinary Nanoscience Center (iNANO), Aarhus University, DK-8000 Aarhus C, Denmark; yin.wang@post.au.dk

* Correspondence: liub@sdut.edu.cn (B.L.); dong@inano.au.dk (M.D.)

Received: 6 February 2018; Accepted: 9 March 2018; Published: 12 March 2018

Abstract: The integration of graphene-based material and TiO₂ can greatly enhance the photodegradation efficiency toward contaminants in the environment. As the morphology of TiO₂ varies from a 0D nanoparticle (NP) and a 1D Nanotube (NT)/Nanowire (NW) to a 2D nanosheet, the contact between TiO₂ and graphene-based material would increasingly intensify and the distribution of TiO₂ on the graphene sheets becomes more uniform. Both factors lead to better photocatalytic performance. The graphene commonly possesses the intrinsic properties of higher surface area, more efficient charge transfer, inhibited electron-hole pairs (EHPs)' recombination and extended light absorption range. With the assistance of some functional surfactants, the photodegradation performance can be further improved according to more specific requirements such as the photodegradation selectivity. This paper provides an overview of recent progress regarding the method and mechanism of graphene in various TiO₂/Graphene composites.

Keywords: TiO₂/Graphene composite; photocatalysis; electron-hole pair; photodegradation

1. Introduction

In the modern scenario of research interests, solutions to climate change and the greenhouse effect appear to be the most investigated field in the scientific community, which can be attributed to the burning of fossil fuels. Innovations to convert from fossil fuels to sustainable and renewable energy sources such as wind, solar, wave and biomass is a high priority. Among these energy sources, solar energy stands out as a favorable choice because it has applications in a broad range of fields such as solar photovoltaic, waste water treatment, solar water heating, etc. Photocatalysis, based on sustainable utilization of a semiconductor and solar energy, is regarded as one of the ideal green solutions to the global energy crisis and environmental deterioration. Almost all of the organic contaminants in the environment can be degraded by photocatalysts with no waste resources or additional pollution. In a typical photocatalytic process, semiconductors can absorb and utilize solar energy because of their featured electronic structure as filled valence band (VB) and empty conduction band (CB). Upon solar light irradiation with energies superior to band gap, electrons will be excited from VB to CB, thus leaving holes in VB. The photogenerated holes and electrons can be utilized to oxidize organic contaminants or reduce water, respectively. Such an innovative way of utilizing solar energy to photocatalyze chemical reactions is effective, low cost and most importantly, environmentally benign.

Among lots of semiconductors that can be employed to photodecompose organic pollutants, titanium dioxide (TiO₂) has been one of the functional materials that are intensively studied, based on

its application in the degradation of contaminants in the environment [1–4]. TiO₂ possesses several benefits, including being a low cost, abundant resource with long term stability, non-toxicity and photocorrosion resistance. On the contrary, the photocatalytic performance of TiO₂ is largely restricted by the wide band gap up to 3.2 eV for the anatase phase, which can only be overcome by the UV light. Upon irradiation, photogenerated EHPs are formed, that are intensively involved in the subsequent photocatalytic reactions. Nonetheless, the EHPs have an extremely short recombination time on the order of 10^{−9} s, which have an adverse effect on photocatalysis. Shortly speaking, TiO₂ is susceptible to adverse charge carrier recombination and low solar energy utilization efficiency. One important strategy among the many proposed solutions is to utilize metal or nonmetal doping into TiO₂ [5–8]. This strategy effectively inhibits the recombination of EHPs and extends the photoresponsive light absorption region. Based on this understanding, composites of graphene and TiO₂ have shown favorable enhancement of photocatalytic efficiency in a lot of studies because of the efficient way in which graphene can transfer charge carrier.

There have been reports on the composites of TiO₂ and various carbon allotropes, which are able to exhibit more enhanced photocatalytic performance compared to bare TiO₂. Graphene, as a shining star of carbon allotropes, owns many unique features. Its two-dimensional lamellar structure endows itself with promising thermal, mechanical, electrical and optical properties. These novel and beneficial properties are utilized in synthesizing graphene-based materials for a variety of technological applications such as nanoelectronics, H₂ production and storage, supercapacitors and catalysis. Incorporation of graphene with TiO₂ would generate a hybrid nanocomposite that integrates desirable properties of each component for targeted applications [9–15]. Consequently, the photocatalytic efficiency of TiO₂ will be improved.

Many cases have indicated that graphene can significantly enhance the photodegradation of pollutants compared to bare TiO₂. To this purpose, recent progress regarding the method and mechanism in TiO₂/Graphene composite is summarized in this review (Table 1). Based on the morphology and constituents in the composite, the review is divided into three main sections. Section 2 introduces TiO₂/Graphene composite with various dimensional morphologies. A series of dimensional morphology will be presented, from 0D NP to a 3D hierarchical nanosphere. Different morphology will cause the change of electron conductivity and reactant absorptivity in the composite. Section 3 focuses on TiO₂/Graphene composite with novel construction or additives. Several surfactant or functional molecules are introduced in the composite to either assist in shaping a novel structure or bringing new features to enhance photoactivity. Section 4 summarizes the common conclusion on the mechanism of graphene-enhanced photodegradation efficiency.

In principle, graphene is a two-dimensional sheet of graphite arrayed hexagonally with monolayer thickness. One fact that needs attentions is that there are ambiguities going through the research references on the nomenclature of graphene and its derivative materials. A certain number of “graphene” referred in the research articles possess actually multiple stacking layers and gradually the term “graphene” has extended to misleadingly stand for a wide range of graphene’s derivatives. It is necessary that a consistent nomenclature is designated and was the theme of another article [16]. This current paper applies the nomenclature regarding graphene terms proposed by the above authors, of which the relevant contents are listed in Table 2. In fact, the term “graphene” should be defined as the isolated monolayer with carbon atoms bonded in the sp² configuration, forming a hexagonal arrangement. The term “Graphene oxide” (GO) refers to the exfoliated form of graphite oxide. Reduced graphene oxide (rGO) means the reduction of GO. We refer to the many derivatives of the graphene family, in this current paper, as “graphene-based materials”.

Table 1. Characterizations of TiO₂/Graphene photocatalysts and their photodegradation performance.

[Ref.] Catalyst Abbreviation	Chemical to Be Degraded	Photocatalytic Activity	Surface Area (m ² /g)	Light Source	Band Gap (eV)	Active Radical
[17] TiO ₂ /Graphene	Benzene & MB	much higher than that of bare TiO ₂		UV& visible light(with a UV cutoff filter, $\lambda > 400$ nm)	2.83	hydroxyl radical & superoxide redical
[18] TiO ₂ /rGO	Arsenite	much the same as Pt/TiO ₂	51.9	$\lambda \geq 320$ nm		superoxide & OH radicals
[19] TGH	MB	complete degradation within 30 min	267.98	UV, centered at 365nm		
[20] TiO ₂ /rGO	MB	photothermal effect contributes ~38% degradation		xenon lamp with a 720 nm short-path filter and a 720 nm long pass filter		
[21] TiO ₂ /GO	MO	improved performance than P25		$\lambda > 400$ nm	2.43	
[22] TiO ₂ /GO	RhD B	a three-fold photocatalytic enhancement over P25	190	mercury lamp		
[23] TiO ₂ /GO	MB	92% MB degraded after 110 min irradiation		mercury lamp		
[24] TiO ₂ /rGO	RhD 6G	more than triple higher photodegradation rate than P25		mercury lamp $\lambda > 400$ nm	2.71	•OH radicals
[25] TiO ₂ spindle/rGO	MG	a 6 fold increase in efficiency over the native TiO ₂ cube	89.34	mercury lamp $\lambda \geq 420$ nm	2.91	
[26] TiO ₂ NW/GO	MB	much higher than TiO ₂ NP/GO and pure TiO ₂ NWs or NPs		solar light		
[27] TiO ₂ nanosheet/Graphene	RhD B & 2,4-dichlorophenol	95% dyes degraded within 60 min		mercury lamp centered at 365 nm		•OH & O ₂ ^{•-}
[28] TiO ₂ nanosheet/rGO	MB	higher than that of TiO ₂		mercury lamp		•OH radicals & holes
[29] TiO ₂ hollow sphere/GO	RhD B	95% degraded within 60 min		mercury lamp	2.51	hydroxyl radicals
[30] TiO ₂ /Graphene	MB & estradiol	2 fold higher photocatalytic activity than TiO ₂		xenon lamp, centered at 350 nm	2.95	

Table 2. Nomenclature used for graphene family materials.

Material	Abbreviation	Formulation
graphene		two-dimensional sheet of graphite arrayed hexagonally with monolayer thickness
graphite oxide		oxidized graphite with oxygen functional groups on the basal planes and increased interlayer spacing
graphene oxide	GO	exfoliated form of graphite oxide
reduced graphene oxide	rGO	reduced form of graphene oxide via a chemical, thermal, solvothermal etc. process

2. TiO₂/Graphene-Based Materials with Various Dimensional Morphologies

2.1. 0D TiO₂ NP/2D Graphene/GO/rGO Sheet

2.1.1. Graphene/GO/rGO Sheet-Spherical TiO₂ NPs

Graphene has many unique features, such as high electron mobility, theoretically high surface area and good mechanical strength. Therefore, it is a plausible assumption that the integration of TiO₂ with graphene could lead to a much improved photocatalytic performance compared with bare TiO₂. Graphene oxide (GO) has a surface decorated with oxygenated functional groups, which provides efficient binding sites for TiO₂. The introduction of GO can act as an electron scavenger and subsequently transport the electrons in an efficient pathway. In addition, the existence of GO enhances the capacity of the hybrid for the physisorption, as well as the chemical adsorption, of degradable molecules. Many cases indicate the photocatalytic effect of TiO₂/Graphene composite. Hiskia et al. reported that, under solar light irradiation, TiO₂/GO presented the same level of photocatalytic activity with commercialized TiO₂ powders (Degussa P25) [31]. Likewise, Xu et al. have fabricated the nanocomposites of TiO₂/Graphene with a series of weight ratios of graphene via a hydrothermal treatment. The as-made TiO₂/Graphene nanocomposites were utilized to photocatalyze the degradation of gas-phase benzene, a volatile organic pollutant (VOC) in air. It was demonstrated that the photocatalytic activity decreased with the weight ratio of graphene [17]. The similar phenomenon was reported by Choi et al. They fabricated a TiO₂-based nanocomposite coupled with reduced graphene oxide (rGO), which led to an efficient photocatalytic oxidation of As(III). The investigation of competitive radical quenchers confirmed that As(III) photocatalytic oxidation was carried out through both superoxide and OH radicals [18]. Bahamode et al. demonstrated the TiO₂/GO composite they prepared with a significantly improved photocatalytic activity with respect to TiO₂ P25 under visible light. A shorter reaction time for photodegradation of 50% pesticides and higher chloride formation rate were achieved with TiO₂/GO [32].

Besides the above-mentioned role of graphene as scavenger and transfer media for electrons, GO has the ability to form a 3D structure through various connections including hydrogen bonding, electrostatic force and π - π electron coupling. Liu et al. fabricated a TiO₂ NPs-graphene hydrogel (TGH) (Figure 1) by a hydrothermal process. The as-prepared TGH possessed 3D interconnected networks and high surface area, which displayed a synergistic effect of the self-assembled TiO₂ NPs and graphene nanosheets. The 3D structure of TGH could significantly enhance the adsorption capacity including physical adsorption and the aromatic dye's adsorption on the surface of graphene via π - π electron coupling. In addition, the 3D graphene networks could transfer electrons efficiently, leading to a significantly improved photocatalytic activity of methylene blue (MB) (Figure 1d) [19].

On the specific function of graphene in photoresponse, Wu et al.'s work clarified that the assumption of up-converted photoluminescence (PL) from rGO excited by noncoherent light was artificial [33]. Therefore, it is disputable to attribute enhanced photocatalytic degradation to the up-converted PL. Except the three common traits of rGO in the process of graphene-based

semiconductor photocatalysis, which are trapping and transferring of photogenerated charges, increasing adsorption of contaminants and extending light absorption, Wu et al. proposed that the strong photothermal effect (PTE) of rGO is another essential factor influencing the photocatalytic performance. In the study on the degradation of MB, the contribution coming from the PTE in the P25/rGO nanocomposite can be as high as 38% except the common advantages of rGO, as shown in Figure 2b,c. Near infra-red irradiation heats up the rGO sheets because of PTE, which renders a faster movement of electrons with more energy on the hot rGO sheets. As a result, PTE facilitates the photodegradation of contaminants in the TiO₂/rGO nanocomposites. Their work indicates that the PTE is of crucial importance in the photocatalysis by graphene-based nanocomposite [20].

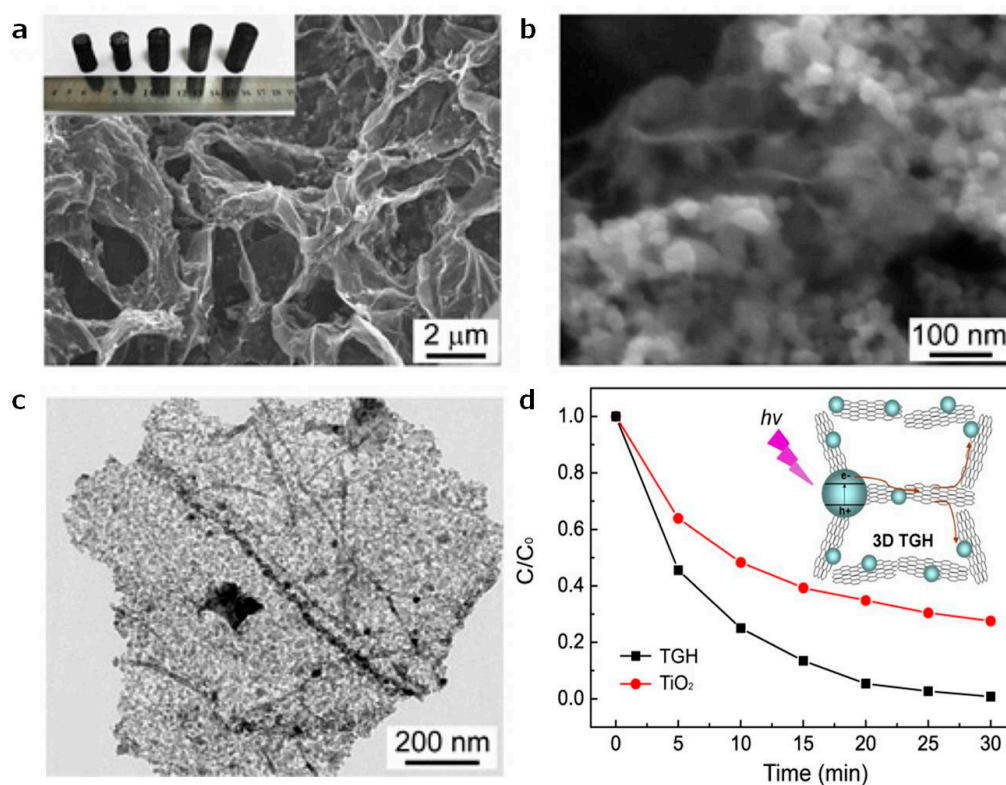


Figure 1. Low- and high-magnified SEM images of TGH (a,b), inset of (a) is the photograph of TGH with a different ratio of TiO₂ to graphene, (c) low-magnified TEM images of TGH. (d) relative changes of the adsorption peak intensity as a function of irradiation time in the presence of TGH and TiO₂ nanoparticles. Inset is the schematic diagrams for illustrating the charge transfer behavior at interfaces in 3D TGH networks. (Reprint from [19] with permission from the American Chemical Society. Copyright 2013).

Normally, the oxidation of graphene can open an electron energy gap, of which the value is determined by the oxidation degree and species of oxygen-containing groups. In this regard, GO could tune its electron conductivity by changing the oxidation degree, which leads to a diverse energy gap and structure distortion and then renders various chemical properties of graphene. Cai et al. studied the influence of the concentration of GO on the photocatalytic activity of TiO₂/GO composite. When the TiO₂/GO hybrid was used to decolorize methyl orange (MO), it was excited by visible light irradiation (>400 nm), that is, both TiO₂ and semiconductor formed by GO could be excited. It was concluded that a narrow band gap as 2.43 eV in the semiconductor formed by GO was a key factor in the photocatalytic activity of the TiO₂/GO hybrid. To be more specific, the p-type semiconductor formed by GO in hybrid with a lower carbon weight ratio in the range of 0.13–0.15 wt % may function as a sensitizer to enhance the photocatalytic performance. Otherwise, higher carbon element changes the GO to an n-type semiconductor and the photocurrent generated was negligible

and the enhancement of photocatalytic performance was not obvious. Their work suggests a possibility of tuning photocatalytic performance by varied C/O ratio in the initial compositions of solution [21].

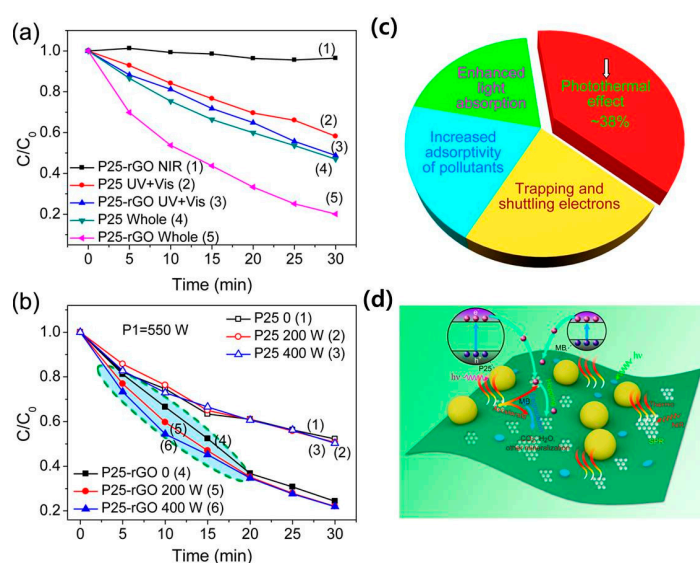


Figure 2. (a) Photocatalytic degradation of MB on P25 or P25-rGO; (b) photocatalytic degradation illuminated by two lamps, lamp 1 with a fixed power provides light in the whole wavelength range and the power of lamp 2 (NIR) is varied; (c) contribution of graphene in the enhanced photocatalytic activity; (d) mechanism of MB degradation over P25-rGO (Reprint from [20] with permission from the American Chemical Society. Copyright 2014).

The TiO₂ nanocrystal growth on graphene sheets is another interesting aspect of TiO₂/Graphene hybrid research. By controlling nucleation and growth, TiO₂ nanocrystals with exposed high active facets could favorably bond to and interact with graphene sheets, thus strengthening the electrical and mechanical coupling within the hybrid. By controlling the rate of hydrolysis, Dai et al. made almost 100% of the TiO₂ nanocrystal grow specifically on the GO sheets, with negligible growth of free TiO₂ nanocrystal in the aqueous solution. The as-prepared hybrid showed remarkably higher photocatalytic activity than other forms of TiO₂ including TiO₂ powders and physical mixture of TiO₂ and GO [22]. To supplement the observation, as exposed high reactive facets can facilitate more active photocatalytic reaction, a TiO₂/Graphene hybrid with exposed {001} facets was prepared by Wang et al. Fabricated via a solvothermal process assisted by the methanol and hydrofluoric acid, the TiO₂/Graphene composites exhibited a superior photocatalytic activity than P25 under UV light [34].

In order to be environmentally benign, Yoo et al. synthesized TiO₂-rGO nanocomposites using a one-step hydrothermal method, with no requirements for toxic solvents or chemicals as a reducing agent for GO. The resulting TiO₂/rGO nanocomposites displayed good photocatalytic activity toward the degradation of Rhodamine B (RhD B) dye under visible light irradiation. In addition, the photocatalytic activity increased with decreasing ratio of rGO in composites [35]. Other endeavors in environmental management include GO membrane separation technology. GO can work as a membrane material due to its good mechanical strength, ultrathin layered structure, excellent flexibility and outstanding separation performance. However, the membrane fouling of GO based membranes is limiting its large-scale application. By photocatalyzing GO membranes, the fouling components—mainly from organic pollutants—can be efficiently removed. Therefore, it is desirable to design a TiO₂/GO composite membrane which can both solve the fouling problem of GO-based membrane and enhance the photocatalytic activity of TiO₂ semiconductor. TiO₂ NPs were in situ grown on the GO sheets and the subsequent UV-light treatment can cause more distinctive wrinkles on the sheet surface, which facilitates molecular transportation. The as-made GO/TiO₂ membrane was utilized in a cross flow filtration process, which displayed outstanding photocatalytic performance

in degradation of MB under UV light. The membrane fouling was efficiently removed with UV light irradiation, leading to a high ability of flux recovery (96%) after 100 min [23].

In 2008, Kamat et al. reported that UV light could be used to effectively reduce GO sheets without a requirement for other reducing chemicals. In the meanwhile, the TiO₂/Graphene composites were simultaneously synthesized with the reduction process going. Likewise, Wei et al. synthesized TiO₂/rGO composites through a facile, reducing chemical-free and UV-assisted photoreduction pathway. By tuning the GO ratio in starting solution and time length of UV irradiation, the dependence on the reduction degree of GO for the photocatalytic activity was investigated. The as-prepared TiO₂/rGO composites displayed better performance in photodegradation of rhodamine 6G (RhD 6G) than the commercial P25 NPs. The better performance of TiO₂/rGO composites was ascribed to the beneficial synergistic effect of graphene and TiO₂ NPs. Beside the common features introduced by graphene, the authors provided several other reasons for activity enhancement. 1. The hydrophilic nature of the functional groups on rGO made TiO₂/rGO composite disperse well in the liquid phase; 2. Strong interaction between the components prevented TiO₂ from leaching out; 3. The efficient desorption of product decomposed from RhD 6G due to the strong oxidization ability of free •OH radicals results in an efficiently recovered graphene surface and the active sites [24].

The above research about TiO₂/Graphene for catalytic degradation of organic pollutants focus on photon-excited degradation. However, the study concerning TiO₂/rGO as a non-light-driven advanced oxidation processes (AOP) catalyst is a rare case. Wang et al. have developed a facile hydrothermal procedure to synthesize TiO₂ NPs and graphene composites. The as-prepared nanocomposite can be used as effective non-light driven catalysts for activating H₂O₂ in oxidative degradation of MB in dark thermal reaction. Using H₂O₂ as an intermediate, MB was effectively degraded by TiO₂/rGO without any light and only 4% of initial MB remained in the solution after 1 h. The mechanism investigation revealed that •OH radicals played a key role in the oxidation pathway [36].

2.1.2. Spindle-Like TiO₂ NP/Graphene/GO/rGO Sheet

Spindle-like TiO₂ NP is another interesting structure in the TiO₂/Graphene composites. Devi et al. demonstrated the conversion of TiO₂ anatase nanocube to anatase nanospindle, while maintaining the bonding between TiO₂ and graphene. The as-formed TiO₂ nanospindle exposed both {001} and {101} facets. The shape transition occurs as a function of reaction duration using TiO₂ cube/GO suspension as a start via a hydrothermal treatment method. With 5% GO loading and a 4h reaction time, the shape transition from nanocubes to nanospindles achieved the maximum limit. TiO₂ spindle/rGO displayed outstanding photocatalytic activity with ~6 times increase compared to respective TiO₂ cube, the reason of which was ascribed to the synergistic effect of more exposed {001} high energy facets and optimized loading of rGO. The rGO sheets made the photoelectrons more separated from the {101} reductive sites and restricted their recombination [25]. A nonstoichiometric spindle-like TiO₂ NP/graphene sheet nanocomposite was prepared by the one-pot thermal hydrolysis of suspension. The direct interaction between TiO₂ nanospindles and graphene sheet led to an anti-restacking property of the exfoliated sheets of graphene. The highest photocatalytic activity of TiO₂/Graphene nanocomposites was achieved with a graphene dopant concentration of 0.002%. The dynamics ceased as an increasing graphene dopant concentration [9].

The above cases suggest that graphene can introduce a series of benefits to the TiO₂ photocatalyst, including efficient electron migration, more reactant adsorptive surface area and a narrowed band gap. But there still exists limitation with TiO₂ NP/graphene sheet morphology, due to the fact that TiO₂ NPs are prone to agglomeration, even forming a dense layer, which certainly reduces the photodegradation activity. Therefore, more research interests aim at constructing TiO₂/Graphene composite with more dimensional morphologies.

2.2. 1D TiO₂ Nanotube (Nanowire)/2D Graphene/GO/rGO Sheet

TiO₂ NPs are susceptible to aggregation and bond poorly to the graphene sheet owing to their almost spherical shape. Compared with TiO₂ NPs, 1D TiO₂ nanotubes (TNTs) have much higher

inner and outer surface area, so as to be rich of active sites. In addition, 1D morphology provides more intimate interfacial contact associated between TNTs and graphene, which should facilitate photogenerated charge separation and subsequently lead to an enhanced photocatalytic activity. Balkus Jr. et al. reported a facile growth of TNTs on rGO sheets via a hydrothermal method. While TNTs were growing on the GO surface, it was observed that GO was simultaneously reduced to rGO. The 1D TNTs on rGO sheets effectively prevented the rGO sheets from agglomeration and made them readily suspending them in aqueous solution. The nucleation and growth of TNTs were assisted by oxygen species on the rGO surface. The as-prepared rGO-TNT composite displayed a much higher photodegradation activity of malachite green (MG) than TNT itself. The optimal loading of rGO was 10% and the much lower and higher additions of rGO led to decreased photocatalytic activity, regardless of UV or visible light irradiation [37].

Analogous to 1D TNT, graphene-1D TiO₂ nanowire (NW) composite (GNW) is an improvement in respect of morphology-related photocatalytic activity. The most distinct advantage using NWs over NPs is that NWs have a closer interfacial contact with graphene sheet, so as to be uniformly grafted onto graphene by simply considering their geometric scenario (Figure 3). Therefore, the photogenerated electron will transfer from TiO₂ to graphene through a very efficient pathway, which promises a higher photocatalytic efficiency. Instead of scattering happening frequently in the NP system, the photogenerated electrons in the NW system gain a direct migration path. According to Fan et al.'s work, TiO₂ NWs were distributed more uniformly on rGO than NPs, therefore more NWs have bonded directly to rGO in contrast to the fact that most NPs do not. Furthermore, in the NW system, charge carriers migrate in a linear path, while in the NP system with agglomeration in most cases, migration occurs in a zigzag path. As a result, electron transfer from NW to rGO can be much more efficient than in agglomerated NPs, which restricts the charge carrier recombination in GNW. A significantly improved photocatalytic activity of GNW nanostructure was proved in the photodegradation of MB under solar light irradiation. A synergistic effect of graphene and 1D NW morphology was proposed to explain the enhanced photodegradation [26]. Based on NW morphology, Li et al. prepared a N-TiO₂ NWs/N-graphene (N-TiO₂/NG) composite by a hydrothermal process utilizing urea as the nitrogen dopant source. N-TiO₂/NG exhibited improved photocatalytic performance under visible light irradiation. The overlap of the N_{2p} energy level of N dopant and the O_{2p} (VB maximum) reduces the energy gap an electron needs to surpass to be injected into CB of N-TiO₂/NG [38].

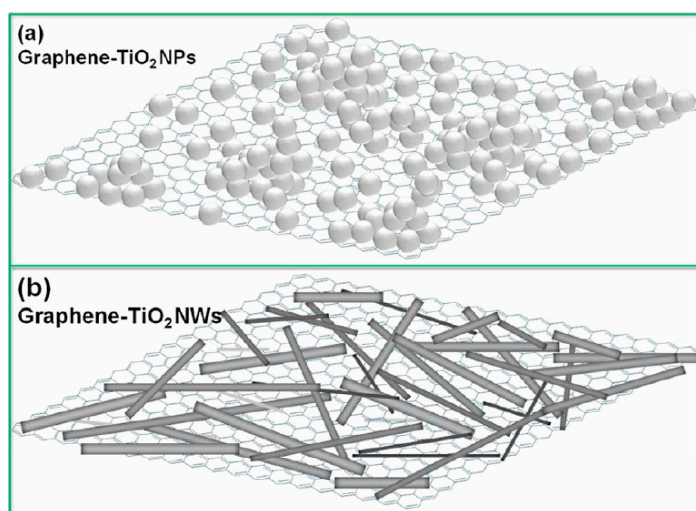


Figure 3. Schematics of (a) TiO₂ NPs agglomerating on graphene sheet and (b) TiO₂ NWs dispersing uniformly on graphene sheet (Reprint from [26] with permission from the American Chemical Society. Copyright 2012).

2.3. 2D TiO₂ Nanosheet/2D Graphene/GO/rGO Sheet

In principle, a 2D–2D heterojunction structure of TiO₂/Graphene composite would favor rapid charge carrier transfer and separation during the photocatalytic process. There were reports of enhanced photoelectrochemical performance because of the stacked TiO₂/Graphene 2D–2D structure. Such 2D–2D layered nanostructures have a maximized contact area between TiO₂ and graphene sheets, which shortens the diffusion path of photoinduced charge carriers, thus facilitating rapid electron transfer across the heterojunction interface. Guo et al. synthesized a TiO₂ nanosheet/graphene-based 2D–2D photocatalytic system, which possessed an intensified electronic and physical coupling effect, leading to efficient electron transfer process and excellent photocatalytic activity toward the degradation of contaminant molecules [27].

Han et al. presented a solvothermal synthesis of graphene-supported anatase TiO₂ sheets. Since rGO sheets can function as a 2D substrate, anatase TiO₂ nanocrystals with exposed {001} high energy facets grew in situ on the rGO surface, in the form of large area 2D sheets. Simultaneously, with the TiO₂ growing on rGO surface, the reduction of GO was successfully achieved. Trapping experiments indicated that the main reason of photocatalytic activity enhancement was attributed to holes left in the TiO₂ crystals other than rapid electrons migrating through rGO [28]. Likewise, Xu et al. fabricated a 2D anatase TiO₂ nanosheets/2D graphene large sheet hybrid. The on-top anatase TiO₂ nanosheets were dominated with high-energy {001} facets as well. Upon visible light irradiation, the as-made nanocomposites exhibited excellent photocatalytic activity. The optimized graphene loading to achieve the highest photocatalytic activity was analyzed to be 1% wt. The Ti atoms on the flat {001} facets are much more exposed, forming sufficient surface defects as oxygen deficiency, which facilitates the interfacial electron transfer and thus effectively separates the photogenerated EHPs. Furthermore, another key factor influencing the enhanced photocatalytic activity is the formation of a chemical Ti–O–C bond, which extends the light absorption band edge to a visible light range [39].

2.4. 3D TiO₂ Hollow Nanospheres/2D Graphene/GO/rGO Sheets

Out of all kinds of nanostructures developed thus far, hierarchical nanostructures are favorable due to their ability of both light scattering with large particles and providing high surface area with small particles. Increased light scattering causes more efficient light absorption and utilization, while high surface area can absorb more contaminant molecules. Another advance of hierarchical structures is the much improved convenience of removing and recycling of photocatalysts. Micro-sized hollow structures are hierarchical structures with properties of large particles, high surface areas and high light utilization. Dong et al. prepared micro-sized TiO₂ hollow spheres (HSs) partially wrapped with rGO bonding through peptide. The hybrid composites were used to reduce 4-nitroaniline (4-NA) under UV and visible light irradiation. A rGO loading with 5% in the composite led to a higher light absorption and reactant adsorption but lower photocatalytic activity than the corresponding composites with 3% rGO loading. This is ascribed to the excessive addition of rGO, which partially shields the primary photoactive TiO₂, and in the meantime, reduces the exposed available TiO₂'s surface-to-light irradiation [40].

Another TiO₂/Graphene composite with similar structure is reported by Zhang et al. Via a solvothermal method, hollow TiO₂ were prepared and subsequently loaded into GO sheet. This hybrid with hierarchical structure was used for the degradation of RhD B under UV and visible light irradiation. The composite exhibited significantly high degradation of RhD B by 75% within 3h, superior to 50% removal efficiency by hollow TiO₂ samples. The GO/hollow TiO₂ hierarchical structure could facilitate the separation of the EHPs and accordingly improve photocatalytic dynamics. Excessive rGO might block TiO₂ active sites and restrict subsequent redox reactions with contaminant molecules. Furthermore, rGO could shield partially the light reaching the TiO₂ surface, which lowered the photon utilization efficiency [29].

3. TiO₂/Graphene-Based Composite with Novel Construction or Additives

3.1. Novel Construction

3.1.1. Hierarchically Ordered Macro-Mesoporous TiO₂-Graphene Films

Jiang et al. synthesized hierarchically ordered macro-mesoporous TiO₂/graphene composite films via a confined self-assembly method (as shown in Figure 4), utilizing polystyrene spheres and pluronic P123 as a macrostructure scaffold and a mesostructured template, respectively. The integration of interconnected macropores in mesoporous films facilitates mass transport across the film, increases the contact area between reactant and the thin film, thus enormously improving their photodegradation activities toward organic dyes. Additionally, the incorporation of graphene into the titania films facilitates the acceptance and transfer of electrons, resulting in the effective suppression of the photogenerated charges' recombination. The electrochemical impedance spectra (EIS) exhibited a shorter semicircle with the component of graphene, which meant a charge-transfer resistance decrease both in the solid-state interface layer and on the surface [41].

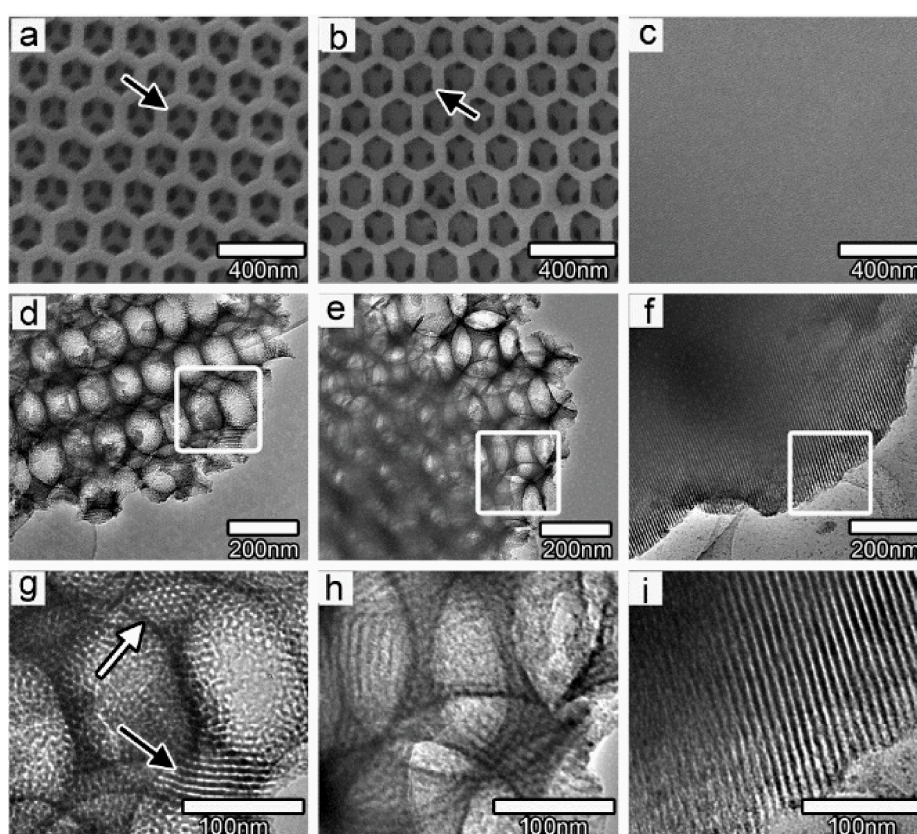


Figure 4. Representative SEM and TEM micrographs of macro-mesoporous titania films. (a,d,g) without graphene; (b,e,h) with graphene; (c,f,i) Representative SEM and TEM micrographs of pure mesoporous titania films (Reprint from [41] with permission from the American Chemical Society. Copyright 2011).

3.1.2. TiO₂/Graphene Nanoflakes

Kim et al. prepared self-assembled TiO₂/rGO nanoflakes via continuous gas-phase synthesis. Compared with P25-TiO₂ NP/ Large rGO, the ultrafine TiO₂ particles gain more access to the rGO nanoflakes. The more intimate contact between the rGO and TiO₂ facilitates efficient electron migration, leading to better photocatalytic performance towards dyes degradation [42].

3.1.3. TiO₂ NP Surrounded by Mono or Bilayer Graphene

Fitri et al. prepared TiO₂/Graphene composites using a direct CVD process. Morphology measurements revealed that the surface of TiO₂ NP is partially surrounded by a mono or bilayer graphene. The formation of thin mono or double layer via CVD process at low temperature was attributed to the ability TiO₂ surface working as a catalyst for aromatization. The TiO₂/Graphene composite displayed increased photocatalytic activity and anti-fouling property compared to the bare TiO₂. Wrapping a graphene layer can also work as a protection layer for the surface of TiO₂ from adsorption by foulant. UV-vis absorption spectra of TiO₂/Graphene composites displayed a stronger absorption in the visible light region compared to bare TiO₂, which can be explained by the π electron of the carbon atom on the TiO₂ surface form Ti–O–C structure, resulting in shifted VB edge and reduced band gap. The low intensity of PL with TiO₂/Graphene composites suggests low recombination rate of the photoinduced EHPs [30].

3.2. With Functional Additives

3.2.1. Graphene Coating of TiO₂ NP Loaded on Mesoporous Silica

Yamashita et al. also developed a graphene coating wrapping TiO₂ NPs hybrid, except they introduced a mesoporous silica as support for the hybrid. TiO₂ NPs exhibited an anatase crystalline structure in the hybrid, while mesoporous silica kept its porous structure as well as the high surface area, after a high temperature carbonization process. Morphology measurement showed that the distribution of TiO₂ NPs anchored on silica was uniform and some ordered hexagonal arrays aligned in the 1D channel after high temperature carbonization. The selective graphene coating increased the adsorption capacity for 2-propanol near the TiO₂ surface anchored on silica. The function of the support, mesoporous silica, is to provide a bonding site for TiO₂ NPs, as well as exhibit no additional diffusion limitation for adsorbed organic molecules [43].

3.2.2. With Floating Autoclaved Cellular Concrete

The small size of TiO₂ particles in powder form makes it difficult to recover used photocatalyst from treated water. In order to develop a photocatalyst with the property of easy recovery and even reuse, a floating autoclaved cellular concrete (ACC), which is an abundant, inert and low cost commercial material, was used to support TiO₂/Graphene composite. The flotation capacity of the nanocomposite enables continuous and extensive contact with the UV radiation and even air oxygen, which are key factors for improving the efficiency of the photocatalytic process. The ACC/TiO₂-GO-8% nanocomposite exhibited relatively good photocatalytic performance in the degradation of three organic compounds and there was no significant release of active component from the ACC support when it was reused in successive cycles [44].

3.2.3. Photocatalytic Reaction with Dye-Sensitization

Dye sensitization can induce electron transfer and this process has been applied on a large scale to increase the photon-to-electron conversion efficiency of solar cells. Upon visible light irradiation, the photogenerated electrons from the excited dye are injected into the anode through semiconductor photocatalysts. Given that the similarity in electron transfer mechanism between dye-sensitized solar cells and photocatalytic reduction of GO, it is a feasible method to apply the dye sensitization mechanism for the reduction of GO. Lei et al. reported such reduction process of GO nanosheets induced by dye sensitization. As shown in Figure 5, the photogenerated electrons are firstly generated on the excited dye molecule and then transferred to the GO via the CB of TiO₂, simultaneously reducing GO to rGO. In order for the electron transfer to process successfully, strong coupling interface between the TiO₂ NPs and rGO is critical, which was evidenced by the difficult detachment of rGO nanosheets from the TiO₂ NPs by ultrasonic dispersion. During the reduction process, a TiO₂/rGO composite was formed. It was shown that the TiO₂/rGO composites displayed superior photocatalytic performance

over pure TiO_2 owing to the effective transfer and separation of photogenerated electrons by rGO nanosheets [45].

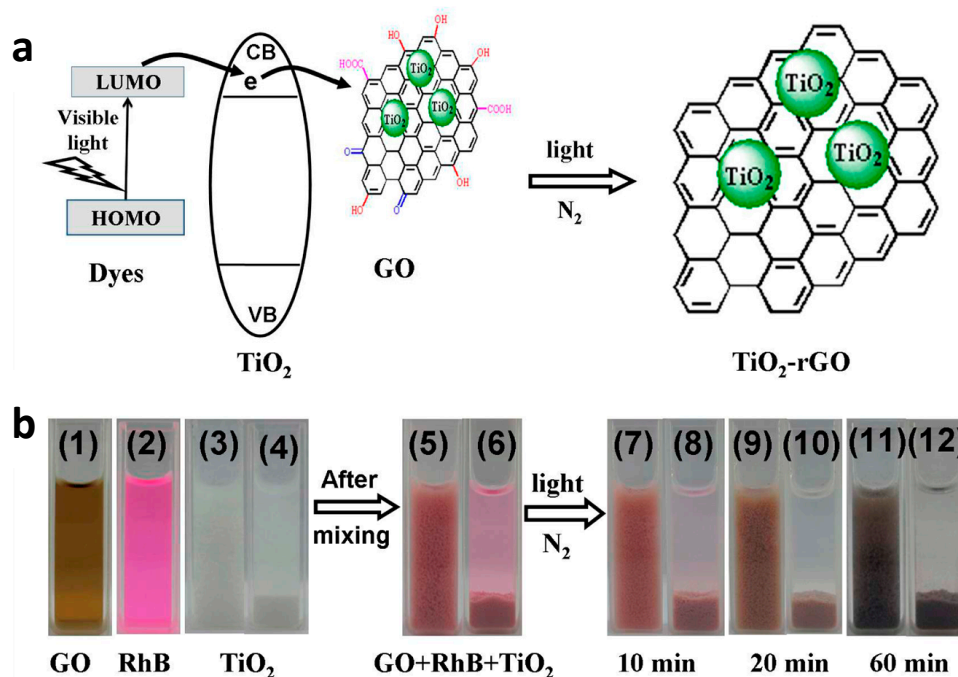


Figure 5. Schematic diagram illustrating the (a) dye-sensitization-induced visible-light reduction of GO nanosheets and the following formation of TiO_2 -rGO composite; (b) photographs of the (1) GO solution, (2) RhB solution, (3, 4) TiO_2 suspension, (5, 6) GO + RhB + TiO_2 mixing solution, (7–12) mixing solution after different irradiation time (Reprint from [45] with permission from the American Chemical Society. Copyright 2013).

3.2.4. Photocatalytic Reaction with a Cu(II) Graft

Transition metal ions, such as Cu(II), have been utilized to promote the multi-electron reduction of O_2 and result in enhancing the photocatalytic efficiency of TiO_2 . Guo et al. reported anchoring Cu(II) on a TiO_2 /rGO mat could lead to an efficient photocatalytic degradation of phenol. Upon UV light irradiation, rGO transfers electrons from photoexcited TiO_2 to the Cu(II) cluster efficiently, which subsequently leads to O_2 multi-electron reduction. Due to the efficient consumption of electrons by Cu(II), more remaining h^+ from excited TiO_2 take part in the subsequent photocatalytic degradation reaction. This process separates photogenerated EHPs and allows them to catalyze respective reactions at separated sites. As a result, rGO and Cu(II) brought in a pronounced improvement in the photocatalytic degradation of phenol. TiO_2 /Cu(II) and TiO_2 /rGO both displayed a decent photocatalytic activity, which can be attributed to efficient molecular oxygen activation by Cu(II) clusters and enhanced charge separation by rGO. The highest photocatalytic activity was achieved with TiO_2 /rGO/Cu(II), indicating a synergistic effect from Cu(II) and rGO [46].

3.2.5. Phenylamine & Tourmaline Functionalization

Photocatalytic degradation can work, in principle, on any kind of dye. So, selective degradation toward a specific dye remains a problem. To solve this problem, many researchers focused on the surface modification of TiO_2 photocatalysts by using specific charged species or polarity molecules to control the surface charge structure. As a result, the dyes with opposite charge can be easily and preferentially adsorbed on the photocatalyst's surface, leading to desirable photocatalytic selectivity. In Yu et al.'s study, negative rGO nanosheets and positive phenylamine (PhNH_2) molecules were loaded at spatially separated loading sites of the TiO_2 surface (as shown in Figure 6). Thus these locally charged sites can be favorable adsorption sites for dyes with opposite charges. The resultant PhNH_2 /rGO- TiO_2

photocatalyst achieved tunable photocatalytic selectivity and realized complete decomposition of dyes both with anionic and cationic charge. Under UV light irradiation, the photogenerated electrons will transfer efficiently to the PhNH₂-modified rGO nanosheets to reduce oxygen. In the meantime, the photogenerated holes staying in the VB of TiO₂ can transfer to the adsorbed anionic dyes to decompose them by oxidation. During the process of H₂O or –OH oxidation by photogenerated holes, the produced hydroxyl radicals can easily diffuse onto the adsorbed cationic dyes on rGO surface, causing the decomposition of cationic dyes [47].

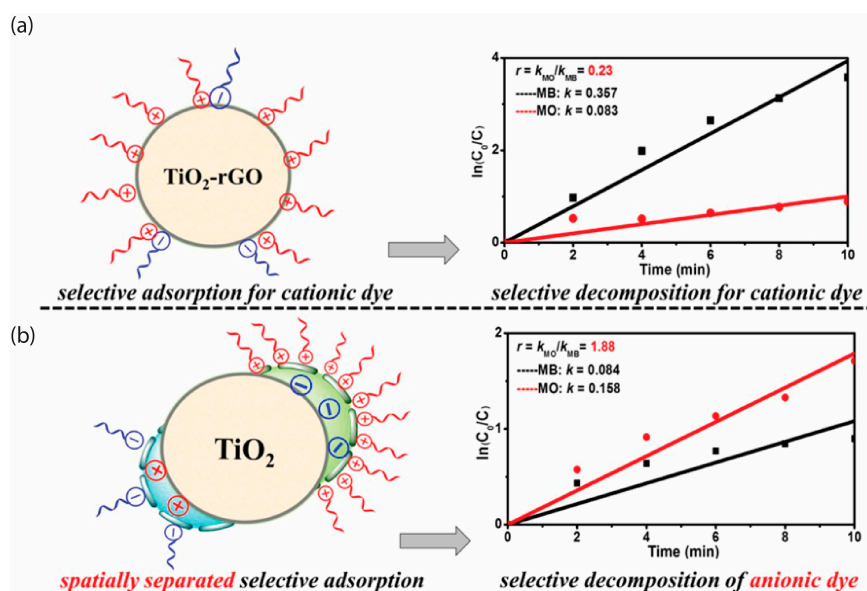


Figure 6. Schematic diagram illustrating (a) the adsorption behaviors of cationic and anionic dyes on TiO₂ surface and corresponding decomposition rate of the MO-MB solutions; (b) the controllable selective adsorption of cationic and anionic dyes and corresponding decomposition rate (Reprint from [47] with permission from the American Chemical Society. Copyright 2016).

Tourmaline is a kind of borosilicate mineral with the electronic directional function. As a result of opposing charges existing at different sites of tourmaline particles, an electric field is present at the surface of tourmaline. Such an electric field favors the photogenerated opposing charges' transportation in the opposite directions. Wang et al. synthesized Graphene/Tourmaline/TiO₂ (G/T/TiO₂) composites via a hydrothermal method. This ternary composite displayed an excellent photocatalytic activity toward degradation of 2-propanol, which was superior to that of the binary systems (G/TiO₂, T/TiO₂) or bare TiO₂. The improved photocatalytic activity was ascribed to the synergetic effect of tourmaline and graphene. Once electrons are photogenerated in TiO₂, graphene can effectively transfer both electrons and holes but in opposite directions, owing to the electronic field of tourmaline. As a result, the recombination of EHPs was greatly restricted. This is evidenced by the PL intensity decrease and the slight blue shift of the PL peak for the G/T/TiO₂ compared with those for TiO₂ [48].

3.2.6. Antibacterial Polyacrylic Coating & Biopolymer

Dispersion of TiO₂ NPs in the matrix of polymers is of importance in respect of practical application. Acrylic polymers can be used as durable outdoor coatings because of their good chemical resistance. The incorporation of TiO₂ with polymers can lead to self-cleaning acrylic coatings. A TiO₂/GO nanocomposite was added to commercial grade polyacrylic latex to obtain a coating with self-cleaning ability and the property of excellent photodegradation. The polyacrylic coatings modified with TiO₂/GO nanocomposites were used to decompose MB and displayed an excellent activity. The optimized weight ratio for TiO₂/GO in the composite was 3% wt, in which the ratio of

TiO₂ to GO was 100:20. In addition, the self-cleaning ability was proved by a water contact angle of 12° after 24 h LED light irradiation, coating stability in water was verified as well [49].

The incorporation of TiO₂ NPs with biocompatible polysaccharides matrix is of interest due to its high mechanical strength, perfect suppleness and better photocatalytic performance. Khan et al. prepared a TiO₂/GO incorporated alginate (Alg)/carboxymethyl cellulose (CMC) nanocomposite via a dissipative convective technique followed by a freeze drying process. Morphological analysis revealed that highly ordered capillaries and pores were present in the composite. Several benefits were realized with such structure including self-organization of microstructure, anti-agglomeration of NPs and uniform dispersion of GO within the nanocomposite. Furthermore, the as-prepared Alg/CMC/GO/TiO₂ nanocomposite displayed better photodegradation toward congo red dye than the Alg/CMC, Alg/CMC/TiO₂ and TiO₂ alone [50].

3.2.7. TiO₂/Graphene Composite with Surfactant & Surface Fluorination

The functionalization of graphene-based material with surfactant is multiple. For example, there were reports about graphene sheets' functionalization by the surfactant molecules [51–53]. The work by Martín-García et al. especially pointed out that the utilization of a zwitterionic surfactant *N*-dodecyl-*N,N*-dimethyl-3-ammonio-1-propanesulfonate (DDPS) was able to improve the reduction efficiency in the reduction process of GO to rGO. Besides, the introduction of DDPS increased the conductivity of rGO without altering the carbon work [51]. As for TiO₂/Graphene-based composite, the modification with surfactant is an effective method to control their morphologies and structures. Xin et al. synthesized a TiO₂/GO nanocomposite with a flower-shaped structure with the assistance of sodium dodecyl benzene sulfonate (SDBS) as the surfactant [11]. In Wu et al.'s work, cetyl trimethyl ammonium bromide (CTAB) was used as a cationic surfactant to synthesize TiO₂/rGO nanocomposite with a novel morphology (Figure 7). Besides, SDBS and Triton X-100 were used as surfactant to regulate the phase structure and morphology of TiO₂/rGO composites as well, leading to TiO₂ NPs and distributed NWs respectively. With array-like TiO₂ nanowires grown on the surface of rGO, TiO₂/rGO-CTAB displayed an excellent photocatalytic efficiency to remove almost all of the MB molecules. Surfactant-assisted hydrothermal method was proved to be an effective approach to improve the structure, morphology and photocatalytic performance of TiO₂/rGO composites [54].

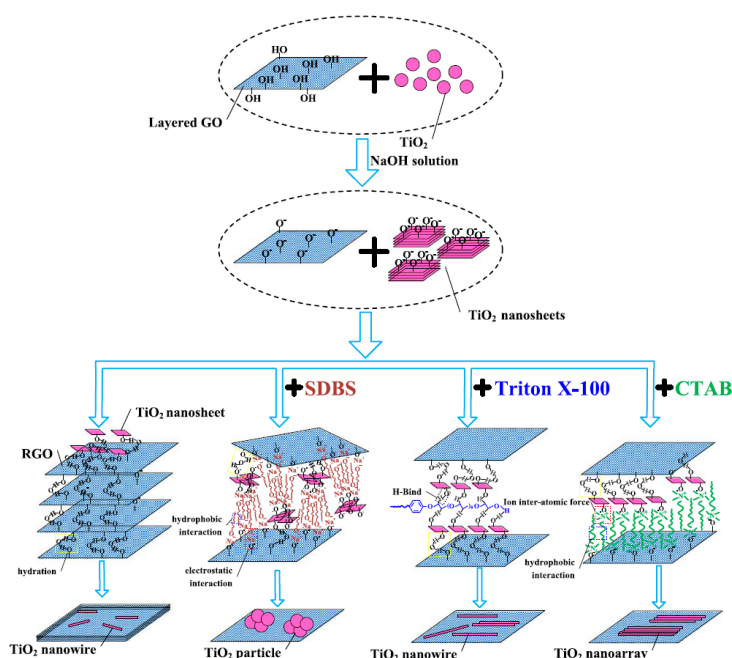


Figure 7. Illustration of the preparation processes and growth mechanism of TiO₂-based nanocomposites (Reprint from [54] with permission from Elsevier. Copyright 2017).

Surface fluorination of TiO₂ is another way of surface modification, which can be completed simply by a ligand exchange between surface hydroxyl groups on TiO₂ and fluoride ions (F⁻). Surface fluorinated TiO₂/rGO (FTG) was synthesized using HF as the source for providing F⁻. The F⁻ ions anchored on the surface of TiO₂ NPs and thus enhanced the crystallization of the TiO₂ anatase phase. The reason for enhanced photocatalytic activity was partly attributed to F⁻ induced favorable crystallization of anatase TiO₂ and the accelerated photocatalytic degradation mediated by •OH radical. The total decomposition ratio of 17β-estradiol over FTG was high—up to 99.8% after a 2 h illumination—while the corresponding value of 17α-ethynyl-estradiol was 99.7% after a 3 h illumination [55].

3.2.8. With Heteroatom Doping

In addition to surface modification, the functionalization of graphene by chemical doping has been applied in photocatalysis as well. Among various heteroatom dopants, the nitrogen doping is an effective way to significantly improve the photocatalytic performance. Three typical N-bonding configurations including graphitic N, pyridinic N and pyrrolic N can be observed. The relationship between N-bonding configuration and the photocatalytic performance of N-doped graphene-based composite was studied by Yu et al. The N-rGO/TiO₂ (N₂H₄), with ca. 63% pyrrolic N and ca. 37% graphitic N-bonding, displayed a 3.63 and 2.64 times higher photocatalytic activity than that of TiO₂ and rGO/TiO₂ respectively. The graphene with graphitic-N configuration functions as an effective electron mediator while the one with pyrrolic-N performs as the oxygen reduction active site [56].

In S-doped TiO₂, the mixing of S_{3p} state with O_{2p} state can cause a defect state in the band gap. S-TiO₂-3D graphene aerogel (3DGA) nanocomposites are prepared via a hydrothermal method followed by a freeze-drying treatment. The as-synthesized S-TiO₂-3DGA catalyst exhibited fairly high photocatalytic activity under the irradiation of UV and visible light. The function of S-doping on the photocatalytic performance was summarized as follows. Firstly, the redshift in the bandgap edge of the S-TiO₂ can decrease the value of band gap, thus extending the light absorption range into the visible region. Secondly, with S dopant, the electron-deficient oxygen could serve as an electron trap to capture electrons, thus reducing the recombination of EHPs [57].

The N,V-TiO₂-rGO was prepared through a facile hydrothermal process, which exhibited much higher visible light photocatalytic activity than bare TiO₂, N-TiO₂ and N,V-TiO₂. The nanocomposites had good stability and their recovery was achieved as well. A N_{2p} state forms due to N doping and overlaps with O_{2p} states, thus lifting the VB top, that is, reducing the band gap. The dopant V would exist in the form of V₂O₅, which is another semiconductor facilitating further extended light absorption [58].

4. Mechanism on Enhanced Photocatalytic Activity by Graphene-Based Material

This paper reviews plenty of research on enhanced photocatalytic activity brought on by incorporation of graphene. With a detailed study on graphene's role from various aspects, there are some common conclusions on one can draw upon. Firstly, as evidenced in reference [22], the TiO₂/GO hybrid has a higher BET surface area (190 m²/g) than both free TiO₂ grown in solution (121 m²/g) and P25 (58 m²/g). In reference [19], a similar enhancement in specific surface area was reported in the TGH due to TiO₂ NPs decoration on graphene nanosheets, so as to partially prevent the aggregation of the graphene sheets. Both the above two cases reported a higher surface area accessible to pollutant molecules in the composite containing graphene, so the amount of physisorption of pollutant molecules is obviously increased. Secondly, the π-π electron coupling between the aromatic region on graphene's surface and aromatic molecules strengthens the interaction with each other [19], further increasing the adsorption of molecules to be decomposed. Thirdly, the excellent electronic conductivity of graphene makes it an ideal electron transfer highway through the interconnected composite, which fastens the separation of photogenerated charge carriers [38] and as a result, inhibits effectively the recombination of EHPs [24,25,30,41]. In Reference [38], Cyclic voltammograms (CV) and EIS measurements were used

to disclose the transfer and separation efficiency of photoinduced EHPs. The hybrid with graphene sheets exhibited large current density, indicating a much increased rate of electron transfer attributed to the introduction of the graphene. $\text{TiO}_2/\text{Graphene}$ exhibited a smaller arc radius in Nyquist diagram than pure TiO_2 , indicating a smaller charge transfer resistance, that is, the fast interfacial transfer and effective separation of photogenerated EHPs at the hybrid interfaces. The PL emission spectra in [24] exhibited a decrease in intensity of PL peak with TiO_2/rGO composites, which attribute to inhibition of the EHPs recombination, thus extending the h^+ existence time. Similarly, in reference [25] the PL intensity was quenched with TiO_2/rGO composite as effective interaction of photo-induced EHPs with the close interfacial contact of rGO sheet, acting as electron acceptor, reduces their radiative recombination. Fourthly, the way of graphene supporting TiO_2 , regardless of the form of NPs or other structures, prevents effectively the aggregation of TiO_2 , thus expanding the exposed TiO_2 surface to a maximum. As a result, the light absorption intensity is absorbed. Finally, because graphene itself can absorb visible light and in the $\text{TiO}_2/\text{Graphene}$ composite, a Ti–O–C chemical bond is formed [30,39], or electronic transitions occur between carbon and TiO_2 phases [59], the light absorption edge is red-shifted from UV to the visible light region, thus narrowing the band gap [9,32,38]. In reference [32] TiO_2/GO catalyst's excellent electronic properties result in excellent photocatalytic behavior under visible light. It was always in the case of TiO_2/GO that a higher initial photo-oxidation rate was achieved compared to that of the commercial TiO_2 P25 material. In reference [38], $\text{TiO}_2/\text{Graphene}$ exhibited a higher MB degradation rate than pure TiO_2 , due to TiO_2 interacted with graphene surface hydroxyl groups, resulting in forming Ti–O–C bonds through hydrothermal reaction.

This knowledge greatly enriches our understanding of graphene's unique function in improving semiconductor photocatalysis, such as TiO_2 . But it does not exclude the possibility that there still exist some disputes regarding graphene's specific property. For example, some scientists believe that a large percentage of enhanced photocatalytic activity should be ascribed to the PTE of graphene instead of other factors. Interesting topics like this will spur more intensive study into the field of graphene-based photocatalysis.

5. Conclusions

The recent progress in the incorporation of graphene with TiO_2 is summarized. As the morphology of TiO_2 component varies from 0D NP through 1D NT/NW, to 2D nanosheet, the contact between TiO_2 and graphene gets more intimate and the distribution becomes more uniform. Both factors facilitate better photocatalytic performance. The graphene's roles are mainly as follows: higher surface area, more efficient charge transfer, inhibited EHPs' recombination and extended light absorption range. With the assistance of some functional surfactant, the photodegradation performance can be further improved according to more specific requirements such as the photodegradation selectivity.

It is worth noticing that the samples we reviewed are mostly suspended functional composites. Recently, another branch of substrate-supported functional composites has attracted lots of attentions. As for such supported system, Raman spectroscopy by itself, or through the combination with atomic force microscopy (AFM) or Rayleigh spectroscopy, emerges as a powerful characterization tool and many insightful conclusions have been obtained [60–68]. Among the above works, several studies involved investigate especially the substrate-supported graphene or few-layer graphene (FLG) systems [60,61]. Caridad et al. studied the inhomogeneities in the charge density of unintentionally doped graphene supported on SiO_2 via Raman spectra; they attributed the doping of graphene to its interaction with substrate other than particle contamination [60]. Besides, the evolution of Raman features is similar to the behavior of suspended graphene [69,70], of which the main conclusion is that the absence of the interaction with a substrate essentially results in an undoped pristine graphene. By utilizing Raman spectroscopy and AFM, Caridad et al. also successfully detect and characterize graphene and FLG in an automated manner. The algorithm they designed provided a basic but robust characterization tool of graphene and FLG in spite of any type of substrate [61]. It is obvious graphene-substrate interaction is one important factor influencing the doping of graphene, or even the

electronic structure of the graphene-based system. By analogy, it is a reasonable expectation that within a supported TiO₂/Graphene composite system, the interaction between substrate and functional composites will play a key role in subsequently determining the photocatalytic and electrochemical behavior. The researches in this promising field will provide more inspirational insights into the TiO₂/Graphene system.

Acknowledgments: We acknowledge the Danish Research Council, AUFF NOVA-project from Aarhus Universitets Forskningsfond and EU H2020 RISE 2016—MNR4SCell project.

Author Contributions: Peipei Huo made her contribution in literature search, design and writing of the whole manuscript. Bo Liu and Mingdong Dong made their contributions in design and editing of the manuscript. Peng Zhao made his contribution in literature search and writing of Section 2 mainly. Yin Wang made his contribution in writing of Section 3 mainly.

Conflicts of Interest: The authors declare no conflict of interest. The founding sponsors had no role in the design of the study; in the collection, analyses, or interpretation of data; in the writing of the manuscript and in the decision to publish the results.

References

1. Ohko, Y.; Luchi, K.; Niwa, C.; Tatsuma, T.; Nakashima, T.; Iguchi, T.; Kubota, Y.; Fujishima, A. 17 β -estradiol degradation by TiO₂ photocatalysis as a means of reducing estrogenic activity. *Environ. Sci. Technol.* **2002**, *36*, 4175–4181. [[CrossRef](#)] [[PubMed](#)]
2. Schneider, J.; Matsuoka, M.; Takeuchi, M.; Zhang, J.L.; Horiuchi, Y.; Anpo, M.; Bahnemann, D.W. Understanding TiO₂ photocatalysis: Mechanisms and materials. *Chem. Rev.* **2014**, *114*, 9919–9986. [[CrossRef](#)] [[PubMed](#)]
3. Lee, J.; Kim, J.; Choi, W. TiO₂ photocatalysis for the redox conversion of aquatic pollutants. *Aquat. Redox Chem.* **2011**, *10*, 199–222. [[CrossRef](#)]
4. Diesen, V.; Jonsson, M. Formation of H₂O₂ in TiO₂ photocatalysis of oxygenated and deoxygenated aqueous system: A probe for photocatalytically produced hydroxyl radicals. *J. Phys. Chem. C* **2014**, *118*, 10083–10087. [[CrossRef](#)]
5. Kuznetsov, V.N.; Serpone, N. On the origin of the spectral bands in the visible absorption spectra of visible-light-active TiO₂ specimens analysis and assignments. *J. Phys. Chem. C* **2009**, *113*, 15110–15123. [[CrossRef](#)]
6. Choi, J.; Park, H.; Hoffmann, M.R. Effects of single metal-ion doping on the visible-light photoreactivity of TiO₂. *J. Phys. Chem. C* **2010**, *114*, 783–792. [[CrossRef](#)]
7. Pan, H.; Zhang, Y.W.; Shenoy, V.B.; Gao, H.J. Effects of H-, N-, and (H, N)-doping on the photocatalytic activity of TiO₂. *J. Phys. Chem. C* **2011**, *115*, 12224–12231. [[CrossRef](#)]
8. Valero, J.M.; Obregón, S.; Colón, G. Active site considerations on the photocatalytic H₂ evolution performance of Cu-doped TiO₂ obtained by different doping methods. *ACS Catal.* **2014**, *4*, 3320–3329. [[CrossRef](#)]
9. Štengl, V.; Popelková, D.; Vlácil, P. TiO₂-graphene nanocomposite as high performance photocatalysts. *J. Phys. Chem. C* **2011**, *115*, 25209–25218. [[CrossRef](#)]
10. Zhu, P.N.; Nair, A.S.; Peng, S.J.; Yang, S.Y.; Ramakrishna, S. Facile fabrication of TiO₂-graphene composite with enhanced photovoltaic and photocatalytic properties by electrospinning. *ACS Appl. Mater. Interfaces* **2012**, *4*, 581–585. [[CrossRef](#)] [[PubMed](#)]
11. Xin, X.; Zhou, X.F.; Wu, J.H.; Yao, X.Y.; Liu, Z.P. Scalable synthesis of TiO₂/graphene nanostructured composite with high-rate performance for lithium ion batteries. *ACS Nano* **2012**, *6*, 11035–11043. [[CrossRef](#)] [[PubMed](#)]
12. Cheng, G.; Akhtar, M.S.; Yang, O.B.; Stadler, F.J. Novel preparation of anatase TiO₂@reduced graphene oxide hybrids for high-performance dye-sensitized solar cells. *ACS Appl. Mater. Interfaces* **2013**, *5*, 6635–6642. [[CrossRef](#)] [[PubMed](#)]
13. Tang, L.A.L.; Wang, J.Z.; Lim, T.K.; Bi, X.Z.; Lee, W.C.; Lin, Q.S.; Chang, Y.T.; Lim, C.T.; Loh, K.P. High-performance graphene-titania platform for detection of phosphopeptides in cancer cells. *Anal. Chem.* **2012**, *84*, 6693–6700. [[CrossRef](#)] [[PubMed](#)]
14. Shiraiishi, Y.; Shiota, S.; Hirakawa, H.; Tanaka, S.; Ichikawa, S.; Hirai, T. Titanium dioxide/reduced graphene oxide hybrid photocatalysts for efficient and selective partial oxidation of cyclohexane. *ACS Catal.* **2017**, *7*, 293–300. [[CrossRef](#)]

15. Li, W.; Wang, F.; Feng, S.S.; Wang, J.X.; Sun, Z.K.; Li, B.; Li, Y.H.; Yang, J.P.; Elzatahry, A.A.; Xia, Y.Y.; et al. Sol-gel design strategy for ultradispersed TiO₂ nanoparticles on graphene for high-performance lithium ion batteries. *J. Am. Chem. Soc.* **2013**, *135*, 18300–18303. [[CrossRef](#)] [[PubMed](#)]
16. Bianco, A.; Cheng, H.M.; Enoki, T.; Gogotsi, Y.; Hurt, R.H.; Koratkar, N.; Kyotani, T.; Monthieux, M.; Park, C.R.; Tascon, J.M.D.; et al. All in the graphene family—A recommended nomenclature for two-dimensional carbon materials. *Carbon* **2013**, *65*, 1–6. [[CrossRef](#)]
17. Zhang, Y.H.; Tang, Z.R.; Fu, X.Z.; Xu, Y.J. TiO₂–graphene nanocomposites for gas-phase photocatalytic degradation of volatile aromatic pollutant: Is TiO₂–graphene truly different from other TiO₂–carbon composite materials? *ACS Nano* **2010**, *4*, 7303–7314. [[CrossRef](#)] [[PubMed](#)]
18. Moon, G.H.; Kim, D.H.; Kim, H.I.; Bokare, A.D.; Choi, W. Platinum-like behavior of reduced graphene oxide as a cocatalyst on TiO₂ for the efficient photocatalytic oxidation of arsenite. *Environ. Sci. Technol. Lett.* **2014**, *1*, 185–190. [[CrossRef](#)]
19. Zhang, Z.Y.; Xiao, F.; Guo, Y.L.; Wang, S.; Liu, Y.Q. One-pot self-assembled three-dimensional TiO₂–graphene hydrogel with improved adsorption capacities and photocatalytic and electrochemical activities. *ACS Appl. Mater. Interfaces* **2013**, *5*, 2227–2233. [[CrossRef](#)] [[PubMed](#)]
20. Gan, Z.X.; Wu, X.L.; Meng, M.; Zhu, X.B.; Yang, L.; Chu, P.K. Photothermal contribution to enhanced photocatalytic performance of graphene-based nanocomposites. *ACS Nano* **2014**, *8*, 9304–9310. [[CrossRef](#)] [[PubMed](#)]
21. Chen, C.; Cai, W.M.; Long, M.C.; Zhou, B.X.; Wu, Y.H.; Wu, D.Y.; Feng, Y.J. Synthesis of visible-light responsive graphene oxide/TiO₂ composites with p/n heterojunction. *ACS Nano* **2010**, *4*, 6425–6432. [[CrossRef](#)] [[PubMed](#)]
22. Liang, Y.Y.; Wang, H.L.; Casalongue, H.S.; Chen, Z.; Dai, H.J. TiO₂ nanocrystals grown on graphene as advanced photocatalytic hybrid materials. *Nano Res.* **2010**, *3*, 701–705. [[CrossRef](#)]
23. Zhu, C.Y.; Liu, G.G.; Han, K.; Ye, H.Q.; Wei, S.C.; Zhou, Y.H. One-step facile synthesis of graphene oxide/TiO₂ composite as efficient photocatalytic membrane for water treatment: Crossflow filtration operation and membrane fouling analysis. *Chem. Eng. Process. Process Intensif.* **2017**, *120*, 20–26. [[CrossRef](#)]
24. Pu, S.Y.; Zhu, R.X.; Ma, H.; Deng, D.L.; Pei, X.J.; Qi, F.; Chu, W. Facile in-situ design strategy to disperse TiO₂ nanoparticles on graphene for the enhanced photocatalytic degradation of rhodamine 6G. *Appl. Catal. B Environ.* **2017**, *218*, 208–219. [[CrossRef](#)]
25. Mukhopadhyay, S.; Maiti, D.; Saha, A.; Devi, P.S. Shape transition of TiO₂ nanocube to nanospindle embedded on reduced graphene oxide with enhanced photocatalytic activity. *Cryst. Growth Des.* **2016**, *16*, 6922–6932. [[CrossRef](#)]
26. Pan, X.; Zhao, Y.; Liu, S.; Korzeniewski, C.L.; Wang, S.; Fan, Z.Y. Comparing graphene-TiO₂ nanowire and graphene-TiO₂ nanoparticle composite photocatalysts. *ACS Appl. Mater. Interfaces* **2012**, *4*, 3944–3950. [[CrossRef](#)] [[PubMed](#)]
27. Sun, J.; Zhang, H.; Guo, L.H.; Zhao, L. Two-dimensional interface engineering of a titania-graphene nanosheet composite for improved photocatalytic activity. *ACS Appl. Mater. Interfaces* **2013**, *5*, 13035–13041. [[CrossRef](#)] [[PubMed](#)]
28. Gu, L.; Wang, J.; Cheng, H.; Zhao, Y.; Liu, L.; Han, X. One-step preparation of graphene-supported anatase TiO₂ with exposed {001} facets and mechanism of enhanced photocatalytic properties. *ACS Appl. Mater. Interfaces* **2013**, *5*, 3085–3093. [[CrossRef](#)] [[PubMed](#)]
29. Zhang, L.; Zhang, J.; Jiu, H.; Ni, C.; Zhang, X.; Xu, M. Graphene-based hollow TiO₂ composites with enhanced photocatalytic activity for removal of pollutants. *J. Alloys Compd.* **2015**, *86*, 82–89. [[CrossRef](#)]
30. Fitri, M.A.; Ota, M.; Hirota, Y.; Uchida, Y.; Hara, K.; Ino, D.; Nishiyama, N. Fabrication of TiO₂–graphene photocatalyst by direct chemical vapor deposition and its anti-fouling property. *Mater. Chem. Phys.* **2017**, *198*, 42–48. [[CrossRef](#)]
31. Fotiou, T.; Triantis, T.M.; Kaloudis, T.; Pastrana-Martínez, L.M.; Likodimos, V.; Falaras, P.; Silva, A.M.T.; Hiskia, A. Photocatalytic degradation of microcystin-LR and off-odor compounds in water under UV-A and solar light with a nanostructured photocatalyst based on reduced graphene oxide–TiO₂ composite: Identification of intermediate products. *Ind. Eng. Chem. Res.* **2013**, *52*, 13991–14000. [[CrossRef](#)]
32. Cruz, M.; Gomez, C.; Duran-Valle, C.J.; Pastrana-Martínez, L.M.; Faria, J.L.; Silva, A.M.T.; Faraldos, M.; Bahamonde, A. Bare TiO₂ and graphene oxide TiO₂ photocatalysts on the degradation of selected pesticides and influence of the water matrix. *Appl. Surf. Sci.* **2017**, *416*, 1013–1021. [[CrossRef](#)]

33. Gan, Z.X.; Wu, X.L.; Zhou, G.X.; Shen, J.C.; Chu, P.K. Is there real upconversion photoluminescence from graphene quantum dots? *Adv. Opt. Mater.* **2013**, *1*, 554–558. [[CrossRef](#)]
34. Jiang, B.J.; Tian, C.G.; Pan, Q.J.; Jiang, Z.; Wang, J.Q.; Yan, W.; Fu, H.G. Enhanced photocatalytic activity and electron transfer mechanisms of graphene/TiO₂ with exposed {001} facets. *J. Phys. Chem. C* **2011**, *115*, 23718–23725. [[CrossRef](#)]
35. Shah, M.S.A.S.; Park, A.R.; Zhang, K.; Park, J.H.; Yoo, P.J. Green synthesis of biphasic TiO₂-reduced graphene oxide nanocomposites with highly enhanced photocatalytic activity. *ACS Appl. Mater. Interfaces* **2012**, *4*, 3893–3901. [[CrossRef](#)] [[PubMed](#)]
36. Li, H.N.; Zhu, M.Y.; Chen, W.; Xu, L.; Wang, K. Non-light-driven reduced graphene oxide anchored TiO₂ nanocatalysts with enhanced catalytic oxidation performance. *J. Colloid Interface Sci.* **2017**, *507*, 35–41. [[CrossRef](#)] [[PubMed](#)]
37. Perera, S.D.; Mariano, R.G.; Vu, K.; Nour, N.; Seitz, O.; Chabal, Y.; Balkus, K.J., Jr. Hydrothermal synthesis of graphene-TiO₂ nanotube composites with enhanced photocatalytic activity. *ACS Catal.* **2012**, *2*, 949–956. [[CrossRef](#)]
38. Liu, C.; Zhang, L.; Liu, R.; Gao, Z.; Yang, X.; Tu, Z.; Yang, F.; Ye, Z.; Cui, L.; Xu, C.; et al. Hydrothermal synthesis of N-doped TiO₂ nanowires and N-doped graphene heterostructures with enhanced photocatalytic properties. *J. Alloys Compd.* **2016**, *656*, 24–32. [[CrossRef](#)]
39. Wang, W.S.; Wang, D.H.; Qu, W.G.; Lu, L.Q.; Xu, A.W. Large ultrathin anatase TiO₂ nanosheets with exposed {001} facets on graphene for enhanced visible light photocatalytic activity. *J. Phys. Chem. C* **2012**, *116*, 19893–19901. [[CrossRef](#)]
40. Wang, X.Y.; Wang, J.; Dong, X.L.; Zhang, F.; Ma, L.; Fei, X.; Zhang, X.; Ma, H. Synthesis and catalytic performance of hierarchical TiO₂ hollow sphere/reduced graphene oxide hybrid nanostructures. *J. Alloys Compd.* **2016**, *656*, 181–188. [[CrossRef](#)]
41. Du, J.; Lai, X.Y.; Yang, N.L.; Zhai, J.; Kisailus, D.; Su, F.; Wang, D.; Jiang, L. Hierarchically ordered macro-mesoporous TiO₂-graphene composite films: Improved mass transfer, reduced charge recombination, and their enhanced photocatalytic activities. *ACS Nano* **2011**, *5*, 590–596. [[CrossRef](#)] [[PubMed](#)]
42. Byeon, J.H.; Kim, Y.W. Gas-phase self-assembly of highly ordered titania@graphene nanoflakes for enhancement in photocatalytic activity. *ACS Appl. Mater. Interfaces* **2013**, *5*, 3959–3966. [[CrossRef](#)] [[PubMed](#)]
43. Kamegawa, T.; Yamahana, D.; Yamashita, H. Graphene coating of TiO₂ nanoparticles loaded on mesoporous silica for enhancement of photocatalytic activity. *J. Phys. Chem. C* **2010**, *114*, 15049–15053. [[CrossRef](#)]
44. Suave, J.; Amorim, S.M.; Moreira, R.F.P.M. TiO₂-graphene nanocomposite supported on floating autoclaved cellular concrete for photocatalytic removal of organic compounds. *J. Environ. Chem. Eng.* **2017**, *5*, 3215–3223. [[CrossRef](#)]
45. Wang, P.; Wang, J.; Ming, T.S.; Wang, X.; Yu, H.G.; Yu, J.G.; Wang, Y.G.; Lei, M. Dye-sensitization-induced visible-light reduction of graphene oxide for the enhanced TiO₂ photocatalytic performance. *ACS Appl. Mater. Interfaces* **2013**, *5*, 2924–2929. [[CrossRef](#)] [[PubMed](#)]
46. Zhang, H.; Guo, L.H.; Wang, D.B.; Zhao, L.X.; Wan, B. Light-induced efficient molecular oxygen activation on a Cu(II)-grafted TiO₂/graphene photocatalyst for phenol degradation. *ACS Appl. Mater. Interfaces* **2015**, *7*, 1816–1823. [[CrossRef](#)] [[PubMed](#)]
47. Yu, H.G.; Xiao, P.; Tian, J.; Wang, F.Z.; Yu, J.G. Phenylamine-functionalized rGO/TiO₂ photocatalysts: Spatially separated adsorption sites and tunable photocatalytic selectivity. *ACS Appl. Mater. Interfaces* **2016**, *8*, 29470–29477. [[CrossRef](#)] [[PubMed](#)]
48. Yin, L.L.; Zhao, M.; Hu, L.H.; Ye, J.H.; Wang, D.F. Synthesis of graphene/tourmaline/TiO₂ composites with enhanced activity for photocatalytic degradation of 2-propanol. *Chin. J. Catal.* **2017**, *38*, 1307–1314. [[CrossRef](#)]
49. Nosrati, R.; Olad, A.; Shakoori, S. Preparation of an antibacterial, hydrophilic and photocatalytically active polyacrylic coating using TiO₂ nanoparticles sensitized by graphene oxide. *Mater. Sci. Eng. C* **2017**, *80*, 642–651. [[CrossRef](#)] [[PubMed](#)]
50. Thomas, M.; Natarajan, T.S.; Sheikh, M.U.D.; Bano, M.; Khan, F. Self-organized graphene oxide and TiO₂ nanoparticles incorporated alginate/carboxymethyl cellulose nanocomposites with efficient photocatalytic activity under direct sunlight. *J. Photochem. Photobiol. A Chem.* **2017**, *346*, 113–125. [[CrossRef](#)]
51. Martín-García, B.; Velázquez, M.M.; Rossella, F.; Bellani, V.; Diez, E.; Fierro, J.L.G.; Pérez-Hernández, J.A.; Hernández-Toro, J.; Claramunt, S.; Cirera, A. Functionalization of reduced graphite oxide sheets with a zwitterionic surfactant. *ChemPhysChem* **2012**, *13*, 3682–3690. [[CrossRef](#)] [[PubMed](#)]

52. Singh, V.; Joung, D.; Zhai, L.; Das, S.; Khondaker, S.I.; Seal, S. Graphene based materials: Past, present and future. *Prog. Mater. Sci.* **2011**, *56*, 1178–1271. [[CrossRef](#)]
53. Xiao, J.; Mei, D.H.; Li, X.L.; Xu, W.; Wang, D.Y.; Graff, G.L.; Bennett, W.D.; Nie, Z.M.; Saraf, L.V.; Aksay, I.A.; et al. Hierarchically porous graphene as a lithium-air battery electrode. *Nano Lett.* **2011**, *11*, 5071–5078. [[CrossRef](#)] [[PubMed](#)]
54. Hu, J.; Li, H.S.; Muhammad, S.; Wu, Q.; Zhao, Y.; Jiao, Q.Z. Surfactant-assisted hydrothermal synthesis of TiO₂/reduced graphene oxide nanocomposites and their photocatalytic performances. *J. Solid State Chem.* **2017**, *253*, 113–120. [[CrossRef](#)]
55. Yang, Y.; Luo, L.J.; Xiao, M.; Li, H.; Pan, X.J.; Jiang, F.Z. One-step hydrothermal synthesis of surface fluorinated TiO₂/reduced graphene oxide nanocomposites for photocatalytic degradation of estrogens. *Mater. Sci. Semicond. Process.* **2015**, *40*, 183–193. [[CrossRef](#)]
56. Xu, Y.; Mo, Y.P.; Tian, J.; Wang, P.; Yu, H.G.; Yu, J.G. The synergistic effect of graphitic N and pyrrolic N for the enhanced photocatalytic performance of nitrogen-doped graphene/TiO₂ nanocomposites. *Appl. Catal. B Environ.* **2016**, *181*, 810–817. [[CrossRef](#)]
57. Chen, Z.P.; Ma, J.F.; Yang, K.; Feng, S.; Tan, W.S.; Tao, Y.X.; Mao, H.H.; Kong, Y. Preparation of S-doped TiO₂-three dimensional graphene aerogels as a highly efficient photocatalyst. *Synth. Met.* **2017**, *231*, 51–57. [[CrossRef](#)]
58. Gu, Y.J.; Xing, M.Y.; Zhang, J.L. Synthesis and photocatalytic activity of graphene based doped TiO₂ nanocomposites. *Appl. Surf. Sci.* **2014**, *319*, 8–15. [[CrossRef](#)]
59. Silva, C.G.; Faria, J.L. Photocatalytic oxidation of benzene derivatives in aqueous suspensions: Synergic effect induced by the introduction of carbon nanotubes in a TiO₂ matrix. *Appl. Catal. B Environ.* **2010**, *101*, 81–89. [[CrossRef](#)]
60. Caridad, J.M.; Rossella, F.; Bellani, V.; Maicas, M.; Patrini, M.; Díez, E. Effects of particle contamination and substrate interaction on the Raman response of unintentionally doped graphene. *J. Appl. Phys.* **2010**, *108*, 085321. [[CrossRef](#)]
61. Caridad, J.M.; Rossella, F.; Bellani, V.; Grandi, M.S.; Díez, E. Automated detection and characterization of graphene and few-layer graphite via Raman spectroscopy. *J. Raman Spectrosc.* **2011**, *42*, 286–293. [[CrossRef](#)]
62. Ferrari, A.C.; Mayer, J.C.; Scardaci, V.; Casiraghi, C.; Lazzeri, M.; Mauri, F.; Piscanec, S.; Jiang, D.; Novoselov, K.S.; Roth, S.; et al. Raman spectrum of graphene and graphene layers. *Phys. Rev. Lett.* **2006**, *97*, 187401. [[CrossRef](#)] [[PubMed](#)]
63. Graf, D.; Molitor, F.; Ensslin, K.; Stampfer, C.; Jungen, A.; Hierold, C.; Wirtz, L. Spatially resolved Raman spectroscopy of single- and few-layer graphene. *Nano Lett.* **2007**, *2*, 238–242. [[CrossRef](#)] [[PubMed](#)]
64. Gupta, A.; Chen, G.; Joshi, P.; Tadigadapa, S.; Eklund, P.C. Raman scattering from high-frequency phonons in supported n-graphene layer films. *Nano Lett.* **2006**, *6*, 2667–2673. [[CrossRef](#)] [[PubMed](#)]
65. Casiraghi, C.; Hartschuh, A.; Lidorikis, E.; Qian, H.; Harutyunyan, H.; Gokus, T.; Novoselov, K.S.; Ferrari, A.C. Rayleigh imaging of graphene and graphene layers. *Nano Lett.* **2007**, *7*, 2711–2717. [[CrossRef](#)] [[PubMed](#)]
66. Sojoudi, H.; Baltazar, J.; Henderson, C.; Graham, S. Impact of post-growth thermal annealing and environmental exposure on the unintentional doping of CVD graphene films. *J. Vac. Sci. Technol. B* **2012**, *30*, 041213. [[CrossRef](#)]
67. Yang, R.; Huang, Q.S.; Chen, X.L.; Zhang, G.Y.; Gao, H.J. Substrate doping effects on Raman spectrum of epitaxial graphene on SiC. *J. Appl. Phys.* **2010**, *107*, 034305. [[CrossRef](#)]
68. Lin, S.S.; Chen, B.G.; Pan, C.T.; Hu, S.; Tian, P.; Tong, L.M. Unintentional doping induced splitting of G peak in bilayer graphene. *Appl. Phys. Lett.* **2011**, *99*, 233110. [[CrossRef](#)]
69. Ni, Z.H.; Yu, T.; Luo, Z.Q.; Wang, Y.Y.; Liu, L.; Wong, C.P.; Miao, J.M.; Huang, W.; Shen, Z.X. Probing charged impurities in suspended graphene using Raman spectroscopy. *ACS Nano* **2009**, *3*, 569–574. [[CrossRef](#)] [[PubMed](#)]
70. Berciaud, S.; Ryu, S.; Brus, L.E.; Heinz, T.F. Probing the intrinsic properties of exfoliated graphene: Raman spectroscopy of free-standing monolayers. *Nano Lett.* **2009**, *9*, 346–352. [[CrossRef](#)] [[PubMed](#)]

